Temperature dependence of phase breaking in ballistic quantum dots

R. M. Clarke, I. H. Chan, and C. M. Marcus
Department of Physics, Stanford University, Stanford, California 94305

C. I. Duruöz and J. S. Harris, Jr.
Solid State Laboratories, Department of Electrical Engineering, Stanford University, Stanford, California 94305

K. Campman and A. C. Gossard
Materials Department, University of California, Santa Barbara, Santa Barbara, California 93106
(Received 8 February 1995)

Ballistic conductance fluctuations are measured in a zero-dimensional (0D) GaAs quantum dot and are used to measure the phase coherence lifetime $\tau_\varphi(T)$ based on a semiclassical "extra lead" model of phase breaking. Above 300 mK, the measured τ_φ decreases as a power law, $\tau_\varphi(T)=a(T\,[K])^{-\zeta}$, with $\zeta\sim 1.2$ and $a\sim 3.5\times 10^{-11}$ s, and appears to saturate below this temperature. Variance of fluctuations increases from zero with dot conductance for few conducting channels in the leads, then saturates once several channels are open. Above 150 mK, variance decreases with temperature as a power law with an exponent between -1.2 and -1.6 depending on $\langle g \rangle$.

Mesoscopic effects such as universal conductance fluctuations (UCF), weak localization, and persistent currents arise from the phase coherence of conduction electrons at low temperatures. The central physical quantity that sets the size and temperature scale for mesoscopic physics is the phase-breaking time τ_φ, that is, the time scale over which the electrons lose phase coherence due to inelastic scattering. At low temperatures, τ_φ may become quite long, allowing electrons to travel several micrometers before phase coherence is lost. In this paper, we will address experimentally the problem of phase breaking in a confined zero-dimensional (0D) system, a GaAs quantum dot.

To date, the majority of work on mesoscopic phenomena have concerned disordered 1D and 2D conductors in which electrons move diffusively through the sample, scattering many times on the time scale of τ_φ. In these situations, well-established methods for extracted phase-breaking rates from transport measurements exist, for instance, using the magnetic-field dependence of weak localization.[1,2] Moreover, the physical mechanisms of phase relaxation in low-temperature diffusive transport are also well understood theoretically,[3] and are generally found to be in good agreement with a large body of experiment in both 2D (Refs. 4–7) and 1D (Refs. 8 and 9) systems.

In micrometer-size quantum dots made from high-mobility two-dimensional electron gas (2DEG) material, the elastic (transport) mean free path may exceed the device size by several times in all directions, so that elastic scattering occurs predominantly as specular reflection at the walls rather than as diffusion. In this case, standard techniques for extracting τ_φ from transport measurements fail. Also, because phase breaking depends on sample dimensionality, one expects a crossover to 0D behavior in small dots. Depending on the context, this crossover to the fully quantized 0D regime is expected as thermal and lifetime broadening become comparable to either the Thouless energy E_c or the single-particle level spacing Δ. Recently, the 0D aspects of phase breaking have been considered theoretically by Sivan, Imry, and Aronov[10] for the case of diffusive electron motion within the dot. We will discuss their results in the context of our experiments below.

From a semiclassical point of view, the power spectrum of magnetoconductance fluctuations can be used to probe the area distribution of electrons traversing the dot.[11–13] The area distribution is influenced by three physical properties of the system: (i) The size and shape of the dot. We will assume chaotic motion of electrons in the dot, in which case only the dot area A is important; (ii) the escape rate from the dot via the leads. This rate is determined by the size of the leads, which can be determined from the average conductance through the dot; and (iii) the phase-breaking rate. Like escape, phase breaking suppresses the contribution of large area trajectories to interference and within the semiclassical model, appears as an "extra lead" for coherent electrons. Together, these three ingredients allow $\tau_\varphi(T)$ to be extracted from conduction fluctuation measurements in a quantum dot.

We discuss data from a total of four quantum dots (Fig. 1 insets), three larger dots (one square and two with protrusions forming Sinai billiards, referred to as Sinai 1 and 2) fabricated from the same GaAs/Al_xGa_{1-x}As heterostructure with mobility 1×10^6 cm^2/V s, and one smaller square dot, fabricated on a lower mobility (1.8×10^5 cm^2/V s) GaAs/Al_xGa_{1-x}As heterostructure. All had sheet densities of $n=3.5\times 10^{11}$ cm^{-2}. The 2DEG interface was 800 Å below the surface for the high-mobility wafer and 420 Å for the other sample. All dots were formed by four independent (Ti/Au) gates and have individually tunable point contact leads in adjacent corners directed at 45° to reduce the probability of

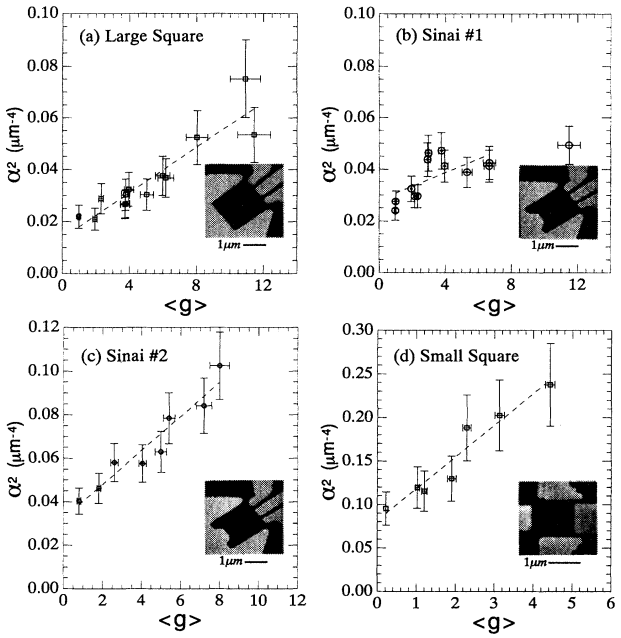

FIG. 1. Characteristic inverse area squared α^2 vs average conductance $\langle g \rangle$ through the dot at base temperature ($T_{\text{fridge}} \sim 20$ mK), from fits of power spectra to Eq. (1). Dashed lines are fits to semiclassical dependence, Eq. (2). Insets are electron micrographs of devices, showing gates (light regions) on the GaAs surface.

straight-through trajectories. Assuming a depletion width of ~ 100 nm between the edge of a gate and the 2DEG, we find the following dot areas A (and corresponding energy-level spacings $\Delta = 2\pi\hbar^2/m^* A$): 2.5 μm^2 (2.8 μeV) for the large square, 2.3 μm^2 (3.1 μeV) for the Sinai dots, and 1.3 μm^2 (5.3 μeV) for the small square. Overall, the three large dots showed very similar fluctuation statistics, and were as different from one another as a given dot was from itself upon thermal cycling. The one small dot exhibited conductance fluctuations on a larger magnetic-field scale, as expected (the exact scaling will be discussed below).

Before discussing the data, we briefly review the semiclassical theory of ballistic conductance fluctuations.[11] A particle in an open chaotic scattering region will remain for a time t with probability $P(t) \propto e^{-\gamma_{\text{cl}} t}$, which defines a classical escape rate γ_{cl}.[14] During that time, the (signed) area traced out by the particle will accumulate diffusively, leading to an approximately exponential distribution of areas $P(A) \propto e^{-2\pi\alpha|A|}$,[11,15,16] where α acts as a characteristic inverse area. In a magnetic field, these areas give rise to a distribution of Aharonov-Bohm fluxes, which modify quantum interference, leading to aperiodic conductance fluctuations. For this $P(A)$, one finds a Lorentzian-squared autocorrelation function of conductance fluctuations,[11] the Fourier transform of which gives the power spectrum,

$$S_g(f) = S_g(0)[1 + 2\pi\alpha\phi_0 f] e^{-2\pi\alpha\phi_0 f}, \quad (1)$$

where f is the frequency in cycles/T and ϕ_0 is the flux quantum (~ 4.14 mT μm^2). The diffusive accumulation of area implies $\alpha^2 \propto \gamma$, where we now use a more general escape rate γ defined in terms of the total transmission through all leads, $\Sigma_c T_c = 2\pi(\hbar\gamma/\Delta)$, with T_c the transmission of the cth lead. For integer number N of fully conducting modes in the cth lead, we may set $T_c = N$, but this definition of γ also holds for partially transmitting modes. The correspondence between γ and γ_{cl} is made by setting N equal to the number of half Fermi wavelengths across the width of the lead.[17]

For well-mixed trajectories, the average conductance through the dot is given by the resistors-in-series form, $\langle g \rangle = 2(T_a^{-1} + T_b^{-1})^{-1}$, where T_a and T_b are the transmissions of the two leads (the factor of 2 accounts for spin degeneracy). For equal lead transmissions, $T_a = T_b$, this gives $\Sigma_c T_c = 2\langle g \rangle$. Even for unequal lead transmissions, $T_a/T_b = \beta \neq 1$, the approximation $\Sigma_c T_c \sim 2\langle g \rangle$ remains quite good. For instance, the fractional error $(\Sigma_c T_c - 2\langle g \rangle)/\Sigma_c T_c = 1 - 4\beta(1+\beta)^{-2}$ for $\beta = 2$ is only 11%.

Phase breaking is modeled as an extra lead of the dot which draws no net current but allows electrons to escape from participating in interference effects.[18–21] The transmission of the phase-breaking lead, T_φ, is defined in terms of the rate $\gamma_\varphi (= 1/\tau_\varphi)$ as $T_\varphi = (2\pi\hbar/\Delta)\gamma_\varphi$. T_φ adds to the transmission via real leads, $\Sigma_c T_c$, to give a total escape rate of phase coherent electrons, $\Sigma_c T_c + T_\varphi = 2\pi\hbar(\gamma + \gamma_\varphi)/\Delta$. The characteristic inverse area α in Eq. (1) is sensitive to coherent electrons and so will scale with this total rate: $\alpha^2 \propto (\gamma + \gamma_\varphi)$. In terms of the average conductance, this scaling can be written

$$\alpha^2 = k[\langle g \rangle + T_\varphi/2], \quad (2)$$

where k is a positive geometry-dependent scale factor inversely proportional to the Fermi velocity, and (within the extra-lead model) independent of temperature.[17] We emphasize that our model assumes that α is only affected by temperature through phase breaking, and not, for instance, by thermal smearing of the Fermi surface. This is supported by recent calculations of conductance fluctuation statistics, which include temperature.[21]

With this model in mind, we now discuss the measurement. Low-field ($B < 0.1$ T) magnetoconductance $g(B)$ was measured in a current-bias configuration using four-wire ac lock-in techniques at 11 Hz, with the voltage drop across the dot kept between 1 and 5 μV. Gates defining the dot shape (Fig. 1 inset) were set to ~ -1 V, then the two point-contact conductances were equalized by setting the conductance of each with the other fully open, before finally closing both. A best-fit cubic polynomial was subtracted from $g(B)$ to remove a slowly varying background conductance, and the power spectrum S_g and variance var(g) were computed from the remaining conductance fluctuations $\delta g(B)$ (Fig. 3 upper inset). The region $|B| < 3$ mT was not used to avoid weak localization contributions.

Characteristic inverse areas α were found by fitting Eq. (1) to the power spectrum of $\delta g(B)$ [Fig. 2(b) inset]. Figure 1 shows α^2 versus average conductance $\langle g \rangle$ at base

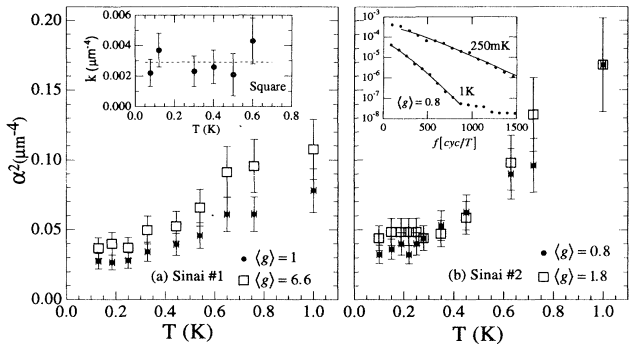

FIG. 2. Characteristic inverse area squared α^2 vs temperature T for the Sinai dots. Two values of $\langle g \rangle$ are shown for each dot. (a) Sinai 1 at $\langle g \rangle = 1$ and $\langle g \rangle = 6.6$; (b) Sinai 2 at $\langle g \rangle = 0.8$ and $\langle g \rangle = 1.8$. Inset left: k at several temperatures for a square dot (dot area was ~10% larger in this run because of the smaller gate voltage used), shows no trend in T. Inset right: Typical fluctuation power spectra showing the change in the slope between 250 mK and 1 K.

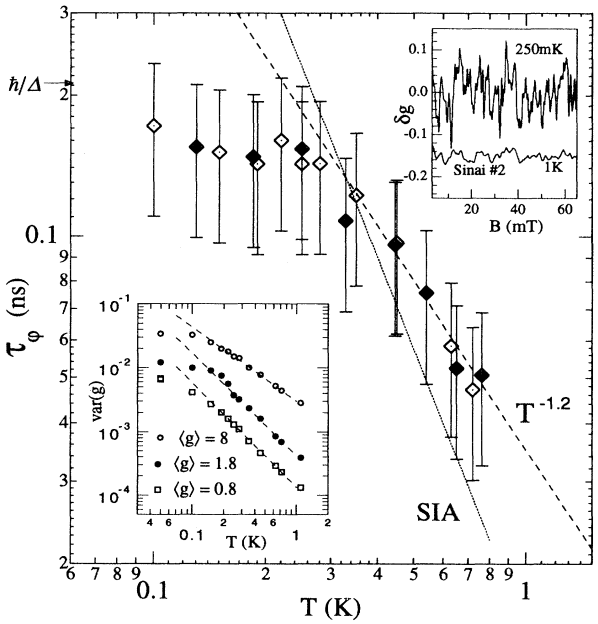

FIG. 3. Phase-breaking time $\tau_\varphi(T)$ extracted from Eq. (3). Dashed line is a two-parameter logarithmic fit to $\tau_\varphi(T) = aT^{-\zeta}$ above 300 mK, giving $\zeta \sim 1.2 \pm 0.5$ for Sinai 1 (solid) and Sinai 2 (open). The dotted line is based on 0D theory (SIA) (Ref. 10). Lower inset: variance of fluctuations var(g) vs T for Sinai 2 at three values of $\langle g \rangle$. Above 150 mK, var(g) $\propto T^{-p}$ with $p \sim 1.6$ for $\langle g \rangle = 0.8$ and 1.8, and $p \sim 1.2$ for $\langle g \rangle = 8$. Upper inset, typical conductance fluctuations $\delta g(B)$ at 250 mK and 1 K (offset downward).

temperature for all four dots. For the large square [Fig. 1(a)], a fit to Eq. (2) gives $k = (4.4 \pm 0.7) \times 10^{-3}$ μm^{-4} and $T_\varphi = 6.1 \pm 1.8$. Using the value of Δ for this dot gives a phase breaking rate of $\gamma_\varphi = (4.1 \pm 1.2) \times 10^9$ s^{-1} ($\hbar\gamma_\varphi/k_B = 32$ mK). For Sinai 1, the fit yields $k = (2.6 \pm 0.6) \times 10^{-3}$ μm^{-4} and T_φ is 11 ± 4, giving a phase-breaking rate $\gamma_\varphi = (8.3 \pm 2.8) \times 10^9$ s^{-1} ($\hbar\gamma_\varphi/k_B = 63$ mK). (The linearity of α^2 versus $\langle g \rangle$ was less apparent in this run for unknown reasons.) The fit for Sinai 2 [Fig. 1(c)] yields $k = (7.4 \pm 1.9) \times 10^{-3}$ μm^{-4} and T_φ of 8.6 ± 3.2, giving a phase-breaking rate of $\gamma_\varphi = (6.5 \pm 2.5) \times 10^9$ s^{-1} ($\hbar\gamma_\varphi/k_B = 49$ mK). For the small square [Fig. 1(d)], α^2 is larger than for the large dots, consistent with the classical scaling with dot area, $k \propto A^{-5/2}$.[16,22] This scaling implies $\alpha^2 \propto A^{-5/2}$ at fixed $\langle g \rangle$ for $T_\varphi \ll \langle g \rangle$, and $\alpha^2 \propto A^{-3/2}$ for $T_\varphi \gg \langle g \rangle$. The fit in Fig. 1(d) yields $k = (3.6 \pm 0.9) \times 10^{-2}$ and $T_\varphi = 4.6 \pm 1.6$, in good agreement with classical scaling. The phase-breaking rate for the small dot is $\gamma_\varphi = (6.0 \pm 2.0) \times 10^9$ s^{-1} ($\hbar\gamma_\varphi/k_B = 45$ mK) comparable to the values found in the larger dots. The rather large uncertainties in T_φ come both from uncertainties in the value of α depending on the frequency range used to fit Eq. (1) and from the estimated error in the fits of α^2 versus $\langle g \rangle$. Uncertainty in dot area further contributes to the estimated uncertainty in γ_φ.

Because the phase-breaking rate increases with temperature, one expects from Eq. (2) that α will also increase with temperature, which is shown in Fig. 2 for the Sinai dots. Using the values of k from above, the measured temperature dependence of α allows T_φ (T), and thus $\tau_\varphi(T)$, to be extracted from Eq. (2). The resulting $\tau_\varphi(T)$ for Sinai 1 and 2 are shown in Fig. 3. For each dot, the values of $\tau_\varphi(T)$ are found from an average of $T_\varphi(T)$ extracted at the two conductances shown in Fig. 2. The assumption that the scale factor k does not itself explicitly depend on T—this follows from the extra lead model of phase breaking—is supported by the measurement shown in Fig. 2(a), though, again, the uncertainties are rather large. That no clear trend in k appears as temperature increases is about the strongest statement one can make given the present data.

Above 300 mK, $\tau_\varphi(T)$ is found to be well described by a power law $\tau_\varphi(T) = a(T\,[\mathrm{K}])^{-\zeta}$ with $\zeta = 1.2 \pm 0.5$ and $a \sim 3.5 \times 10^{-11}$ s as shown in Fig. 3 for the two Sinai dots. The measured $\tau_\varphi(T)$ is consistent in magnitude with a recent calculation by Sivan, Imry, and Aronov (SIA) of the phase-breaking rate in a diffusive 0D quantum dot, $\tau_\varphi^{-1}(T) = (32\Delta/\pi)\Xi(kT/E_c)^2$, where E_c is the Thouless energy and Ξ is a constant of order unity.[10] For our ballistic dots made from 2DEG material, $\Xi = \frac{9}{4}$ and $E_c \sim \hbar v_F/\sqrt{A} \sim 1$ K, giving the line shown in Fig. 3. We also note that our measured $\tau_\varphi(T)$ agrees with previous measurements of phase breaking in a disordered 2D GaAs sample.[4] Below 300 mK, $\tau_\varphi(T)$ appears to saturate between 0.1–0.2 ns. We believe this saturation is not a result of heating within the dot, but rather may reflect a breakdown of our semiclassical model where τ_φ affects the characteristic field scale of fluctuations. This is suggested by the observation that var(g) does not show a corresponding saturation, and continues to increase down to ~150 mK (Fig. 3 lower inset). We note that the saturation (maximum) value of τ_φ occurs at a time compara-

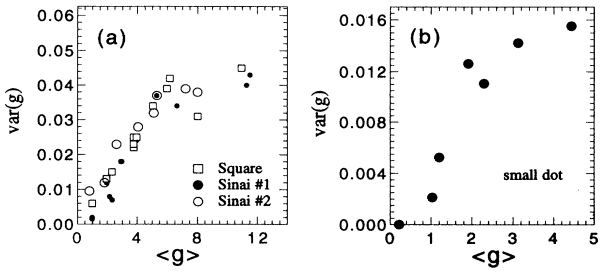

FIG. 4. Variance of fluctuations var(g) vs $\langle g \rangle$ at base temperature ($T_{\text{fridge}} \sim 20$ mK) for (a) the three large dots and (b) the small square dot. Note that var(g) appears to saturate at lower $\langle g \rangle$ for the small dot.

ble to the Heisenberg time $\tau_H \sim \hbar/\Delta \sim 0.2$ ns for these dots, indicated by an arrow on Fig. 3; and one does not expect the semiclassical picture to hold when lifetimes become long compared τ_H. For the entire data range shown, the inequality $\tau_\varphi(T) > \hbar/k_B T$ is easily satisfied.

Finally, we examine var(g) as a function of T and $\langle g \rangle$. For all dots, we find a roughly linear increase in var(g) with $\langle g \rangle$ for small $\langle g \rangle$, as shown in Fig. 4. For the large dots this trend rolls off at var(g)$\sim$0.04 [in units of $(e^2/h)^2$] for $\langle g \rangle \sim 6$, while for the small dot the roll off occurs at var(g)$\sim$0.014 for $\langle g \rangle \sim 3$. In all cases, var(g) is less than the universal value of $\frac{1}{4}$.[23,24] This discrepancy, as well as the strong dependence on $\langle g \rangle$, is presumably associated with both phase breaking and thermal smearing. Within our phase-breaking picture, the saturation in var(g) at larger $\langle g \rangle$ occurs once the number of real escape channels ($\sim 2\langle g \rangle$) dominates the number of phase-breaking channels.

The temperature dependence of var(g) appears well described by a power law above 150 mK, with the power of T showing a dependence on $\langle g \rangle$ (Fig. 3 inset). For smaller conductances, $\langle g \rangle = 0.8$ and 1.8, we find var(g) $\propto T^{-1.6}$; when the leads are more open, $\langle g \rangle = 8$, var(g) $\propto T^{-1.2}$. The latter dependence agrees with previous measurements of UCF in disordered 1D wires.[25,26] This crossover in power law will be investigated further in future work.

We thank B. Altshuler, K. Efetov, Y. Gefen, Y. Imry, and U. Sivan for informative discussions, and Chris Knorr for technical assistance. Research was supported in part by the NSF-MRL through the Stanford Center for Materials Research, by JSEP under Contract No. DAAL03-91-C-0010, at UCSB by the Air Force Office of Scientific Research Contract No. AFOSR-91-0214, and by QUEST, an NSF Science and Technology Center.

[1]B. L. Altshuler, A. G. Aronov, M. E. Gershenson, and Y. V. Sharvin, Sov. Sci. Rev. A Phys. **9**, 223 (1987).
[2]C. W. J. Beenakker and H. van Houten, in *Solid State Physics: Advances in Research and Applications,* edited by H. Ehrenreich and D. Turnbull (Academic, San Diego, 1991), Vol. 44.
[3]B. L. Altshuler, A. G. Aronov, and D. E. Khmelnitsky, J. Phys. C **15**, 7367 (1982).
[4]D. A. Poole, M. Pepper, and R. W. Glew, J. Phys. C **14**, L995 (1981).
[5]M. J. Uren, R. A. Davies, M. Kaveh, and M. Pepper, J. Phys. C **14**, L395 (1981).
[6]For a review of experimental results on 2D films see B. L. Altshuler, A. G. Aronov, M. E. Gershenson, and Y. V. Sharvin, Sov. Sci. Rev. A Phys. **9**, 223 (1987).
[7]D. M. Pooke, N. Paquin, M. Pepper, and A. Gundlach, J. Phys. Condens. Matter **1**, 3289 (1989).
[8]P. M. Echternach, M. E. Gershenzon, and H. M. Bozler, Phys. Rev. B **48**, 11 516 (1993).
[9]J. P. Bird *et al.*, J. Phys. Condens. Matter **2**, 7847 (1990).
[10]U. Sivan, Y. Imry, and A. G. Aronov, Europhys. Lett. **28**, 115 (1994).
[11]R. A. Jalabert, H. U. Baranger, and A. D. Stone, Phys. Rev. Lett. **65**, 2442 (1990).
[12]E. Doron, U. Smilansky, and A. Frenkel, Physica D **50**, 367 (1991).
[13]C. M. Marcus *et al.*, Phys. Rev. Lett. **69**, 506 (1992).
[14]U. Smilansky, in *Chaos and Quantum Physics,* edited by M. Giannoni, A. Voros, and J. Zinn-Justin (Elsevier, Amsterdam, 1990).
[15]M. V. Berry and M. Robnik, J. Phys. A **19**, 649 (1986).
[16]O. Agam, J. Phys. (France) I **4**, 697 (1994).
[17]E. Doron and U. Smilansky, Phys. Rev. Lett. **68**, 1255 (1992).
[18]C. M. Marcus, R. M. Westervelt, P. F. Hopkins, and A. C. Gossard, Phys. Rev. B **48**, 2460 (1993); C. M. Marcus *et al.*, Semicond. Sci. Technol. **9**, 1897 (1994).
[19]M. Büttiker, Phys. Rev. B **33**, 3020 (1986).
[20]M. Büttiker, IBM J. Res. Dev. **32**, 317 (1988).
[21]K. B. Efetov, Phys. Rev. Lett. **74**, 2299 (1995).
[22]R. V. Jensen, Chaos **1**, 101 (1991); R. A. Serota *et al.*, Phys. Rev. B **36**, 5031 (1987).
[23]R. A. Jalabert, J.-L. Pichard, and C. W. J. Beenakker, Europhys. Lett. **27**, 255 (1994).
[24]H. U. Baranger and P. A. Mello, Phys. Rev. Lett. **73**, 142 (1994).
[25]T. J. Thornton *et al.*, Phys. Rev. B **36**, 4514 (1987).
[26]J. R. Gao, A. H. Verbruggen, S. Radelaar, and J. Middelhoek, Phys. Rev. B **40**, 11 676 (1989).

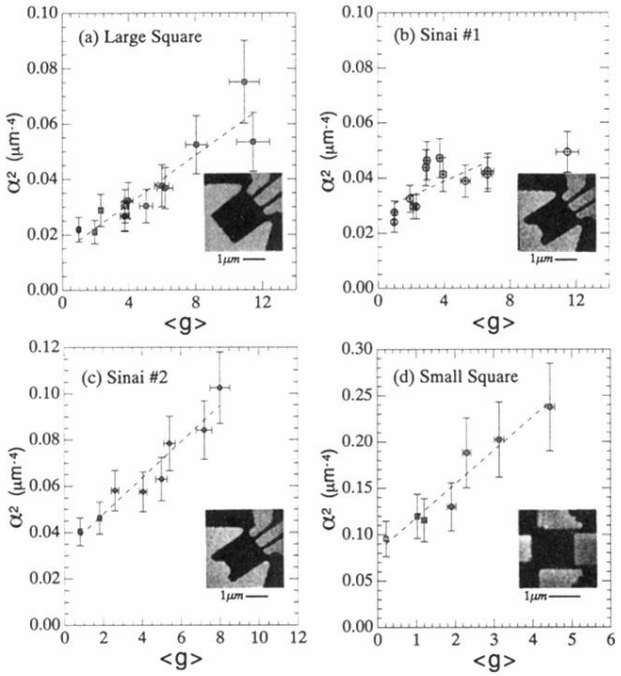

FIG. 1. Characteristic inverse area squared α^2 vs average conductance $\langle g \rangle$ through the dot at base temperature ($T_{\text{fridge}} \sim 20$ mK), from fits of power spectra to Eq. (1). Dashed lines are fits to semiclassical dependence, Eq. (2). Insets are electron micrographs of devices, showing gates (light regions) on the GaAs surface.